

Exploring Neural Biomarkers in Young Adults Resistant to VR Motion Sickness: A Pilot Study of EEG

Gang Li
University of Glasgow
Shanghai Jiao Tong University

Katharina Pohlmann
University of Glasgow

Mark McGill
University of Glasgow

Chao Ping Chen
Shanghai Jiao Tong University

Stephen Brewster
University of Glasgow

Frank Pollick*
University of Glasgow

ABSTRACT

VR (Virtual Reality) Motion Sickness (VRMS) refers to purely visually-induced motion sickness. Not everyone is susceptible to VRMS, but if experienced, nausea will often lead users to withdraw from the ongoing VR applications. VRMS represents a serious challenge in the field of VR ergonomics and human factors. Like other neuro-ergonomics researchers did before, this paper considers VRMS as a brain state problem as various etiologies of VRMS support the claim that VRMS is caused by disagreement between the vestibular and visual sensory inputs. However, what sets this work apart from the existing literature is that it explores anti-VRMS brain patterns via electroencephalogram (EEG) in VRMS-resistant individuals. Based on existing datasets of a previous study, we found enhanced theta activity in the left parietal cortex in VRMS-resistant individuals (N=10) compared to VRMS-susceptible individuals (N=10). Even though the sample size per se is not large, this finding achieved medium effect size. This finding offers new hypotheses regarding how to reduce VRMS by the enhancement of brain functions per se (e.g., via non-invasive transcranial electrostimulation techniques) without the need to redesign the existing VR content.

Keywords: VR motion sickness, brain state problem, EEG, resistance to VR motion sickness.

Index Terms: Neuro-ergonomics, vestibular system, VR motion sickness, cybersickness, EEG

INTRODUCTION

Despite Virtual Reality (VR) technologies becoming widely used commercially since 2016, the problem of VR-induced cybersickness or VR visually-induced motion sickness persists as it affects many scientific fields, including computing science, biomedical engineering, psychology, and neuroscience. In this paper, we refer to this phenomenon as VR motion sickness (VRMS), where VR is the origin of this problem and motion sickness represents the nature of this problem. With VR being the origin of VRMS, it refers to purely visually-induced motion sickness without the involvement of a motion platform in the real world. Also, it specifically refers to consumer head-mounted display (HMD) VR rather than curved monitor VR [1], cave

automatic virtual environments VR [2] as well as its advanced version dome VR [3].

Because obvious VRMS symptoms that can be observable by VR users themselves include racing heartbeat, cold sweat, nausea and other responses from the autonomic nervous system, peripheral physiological signals are straightforward measures to detect VRMS [4]. However, when it comes to the etiology of VRMS, the majority of neuroscientists or neuro-ergonomics researchers accept the notion that VRMS is a brain state problem caused by mismatched visual and vestibular sensory inputs, according to sensory-conflict theory (see Section 2 below) [5]. Particularly, Matthias et al for the first time found a direct association between increasing mismatch levels and subjective VRMS ratings [6], which provided partial supporting evidence for the proposed VRMS etiology. Thus, identifying VRMS-related neural responses using brain imaging techniques like electroencephalogram (EEG) [6]–[10] or functional near-infrared spectroscopy (fNIRS) [11] is also an active research area in VRMS studies.

The current state-of-the-art brain imaging techniques-based VRMS detection involves a participant wearing an HMD VR headset and watching illusory self-motion-inducing VR contents (e.g., traveling in a tunnel or riding a rollercoaster) in a first-person perspective while having their EEG signals monitored. Then, conventional statistics [6], [7] or advanced artificial intelligence (AI) approaches [8]–[10] are employed to find the potential correlates between objective EEG features and subjective VRMS ratings. Both [6] and [7] found that some EEG features in the vestibular regions are significantly associated with VRMS ratings, but [7] made this conclusion based on more comprehensive EEG features and taking peripheral physiological signals as references. Regarding AI-based studies, except for [10], authors claimed that their AI models could achieve a very good detection accuracy of 82.83% with sample size N=130 [8] or even as high as 98% with sample size N=25 [9]. However, as pointed out by [12], a key open question in AI-based studies of brain imaging techniques is always: how to ensure the neural interpretability of those AI decision-making layers if feature visualization was not implemented. In other words, neural interpretability is a key step to investigate the causal links between identified EEG features and VRMS ratings. If this point is ignored, then the AI results will be unable to guide the ensuing development of VRMS mitigation/intervention techniques. Taken together, AI research in the field of VRMS is still in its infancy, and it is combining conventional statistics methods with clear brain research regions which is a rigorous scientific approach worth following.

The present work advances on previous rigorous studies [6], [7], by identifying the differences in EEG-based brain activity patterns between VRMS-resistant and -susceptible young adults. This work aims to determine whether a hypothesis can be

Gang.Li@glasgow.ac.uk
Katharina.Pohlmann@glasgow.ac.uk
Mark.McGill@glasgow.ac.uk
ccp@sjtu.edu.cn
Stephen.Brewster@glasgow.ac.uk
Frank.Pollick@glasgow.ac.uk (*Corresponding Author*)

generated for future neurostimulation studies to develop a novel

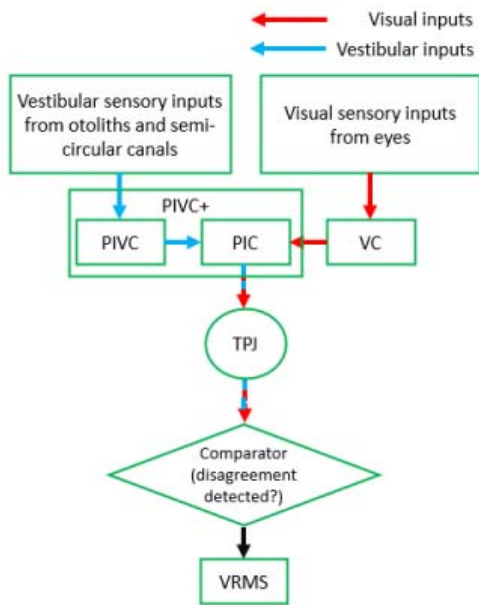


Figure 1: Simplified sensory conflict theory where proprioceptive sensory inputs are ignored. Also, the neural pathway from vestibular sensory organs to the brain is simplified to PIVC only, which may include the cerebellum, brainstem and thalamus as well (see [18]). VC: visual cortex.

brain regulation techniques-based VRMS mitigation solution.

This is a new data analysis study based on partial data from a previous study [7]. The open data set showed after watching the moderate VRMS-inducing contents (that is, tunnel travel), exactly half of the participants (N=10) dropped out due to high VRMS ratings while the other half (N=10) completed to trial. The sex ratios were almost the same in the two sub-groups (7 females and 3 males for those who did not drop out and 8 females and 2 males for those who dropped out). This provided us with a valuable opportunity to further investigate the data to unlock the brain patterns of those who did not drop out. We define them as the VRMS-resistant people here.

We believe that studying those who are relatively resistant to VRMS becomes just as critical as studying those who are suffering from it, because this could offer new insight into the prevention and reduction of VRMS by enhancement of brain functions.

2 THEORY AND PARTIAL NEURAL BASIS

Sensory-conflict theory is a widely-used theory to explain the etiology of motion sickness. Its core content is that motion sickness is the body's response to inharmonious sensory information reaching the so-called comparator in the brain [13]. Here, inharmonious sensory information may come from all three sensory systems for balance control: visual, vestibular and proprioceptive systems. Among them, VRMS is caused by disagreement between visual and vestibular sensory inputs only (as shown in Fig. 1). It does not involve the proprioceptive system as this system is about the sense of one's body position in relation to the things around it, which is associated with traditional passenger motion sickness (where participants are physically moving) rather than visually-induced motion sickness.

Regarding the neural substance of the so-called comparator, it remains unclear, but modern fMRI studies have shown that temporoparietal junction (TPJ) plays a key role in the integration of vestibular and visual sensory inputs [14], [15]. A more recent fMRI study further found that before vestibular and visual sensory inputs are integrated into the TPJ, they already meet in the parietal insular cortex (PIC) — a further divided area from traditional parieto-insular vestibular cortex (PIVC) region [16]. Accompanying the division of the PIC, the traditional PIVC region is now renamed as PIVC+ consisting of two functional areas: 1) a visual-vestibular area, PIC; pa2) a pure vestibular area, PIVC [16]. Thus, in the following sections, PIVC refers to the new PIVC defined in [16].

3 METHODS

3.1 Participants and Datasets

The existing datasets includes a total of twenty young university students (mean age: 22 y/o; range 20-32 years; 5 males). All participants had normal or corrected-to-normal vision, and were self-reported free from neurological/psychiatric disorders. They all reported playing less than 2 hr of PC or VR video games per month. All participants were paid £10/hr for their participation. Participants were required to sit still during a tunnel travel task.

Datasets of these participants can be found here: <https://doi.org/10.5281/zenodo.6373681>

3.2 Experimental Setup and Procedure

Each participant was asked to passively watch a moving tunnel (see more details in section 3.3 below) in a Meta Quest 2 VR HMD while having their EEG signals monitored using a wireless 8-channel research-grade device (StarStim8, Neuroelectronics Inc. Ltd, Spain). The duration of the tunnel travel was set to 10-min. Participants were required to report their sickness ratings every minute on the Fast Motion Sickness scale (FMS) [17] displayed in the VR scene. This scale ranged from 0 to 20 and is a commonly-used short questionnaire for fast online VRMS assessments. We defined VRMS-resistant people as those who could complete the entire 10-min task, while VRMS-susceptible people were defined as those who voluntarily dropped out when they felt they could no longer continue the experiment or forced to quit by the on-site experimenter when their sickness ratings were equal or larger than a pre-defined ethical threshold, that is, 11 (which represented moderate sickness ratings in FMS). The procedure was approved by the ethics panel of the University of Glasgow (No. 300200009), College of Science and Engineering.

This slider was visible at the end of every minute (see Fig. 2), and once the slider was visible, the tunnel would stop (which indicates the end of one trial) until participants finished their ratings. The timing of the end of each trial and the EEG recordings were synchronized using a proven protocol (see section 3.3 below), thus trial-by-trial EEG analysis could be done. Note that unlike offline VRMS assessments that cover more comprehensive VRMS symptoms (e.g., simulator sickness questionnaire (SSQ) covers nausea, oculomotor and disorientation symptoms [18]), FMS only focuses on the most intolerable symptom, nausea. The Meta Quest 2 (72 Hz display refresh rate and 89° horizontal field of view) is an EEG-friendly consumer HMD VR., so was adopted to collect data in [7].

3.3 VRMS-inducing Tunnel Travel

As the name implies, the tunnel travel required the participant to travel in a virtual tunnel, mainly involving the perception of combined linear movements along the z-axis, side-to-side yaw rotation around the y-axis as well as up-down pitch rotation around the x-axis (see Fig. 3). This tunnel travel task was adapted

from [19]. The route was set as a normal driving scenario, including turns (that is, the combined linear movements along the



Figure 2: The screenshot of the tunnel travel scene and digital FMS questionnaire.



Figure 3: The illusory self-motions induced by watching tunnel travel in VR

z-axis and side-to-side yaw rotation around the y-axis), uphill and downhill paths (that is, the combined linear movements along the z-axis and up-down pitch rotation around the x-axis), but without upside down and off-axis paths. Unlike the fixed movement speed in the original version of [19], the movement speed was adjustable in the present study. It was increased by 20% in the second time window if the same FMS score was reported in consecutive 2-min periods, in order to avoid a quick adaptation effect and keep participants always experiencing some level of VRMS. All participants were instructed to focus on the centre of the scene as they were performing this tunnel task.

This task was developed with Unity version 2019.3.14. The synchronization between VR event markers and EEG recordings was implemented by the C# version of the lab streaming layer (LSL) protocol. The LSL protocol, developed by University of California, San Diego a decade ago, can ensure sub-millisecond accuracy as long as both the LSL host (marker sender: Unity) and client (receiver: EEG recording software) are in the same local network. The LSL's applicability in combined VR-EEG settings and has been confirmed in previous studies [20], [21]. The merge of Unity project and LSL was straightforward since the Unity project per se was C# based. What was needed to do was just to call the function named *push_sample (data)* by the end of each trial, where *push_sample ()* is a ready-to-use function in LSL library for sending data from marker sender to receiver, and *data* is the customized markers with the data type of integer.

3.4 Behavioral Data Analysis

The FMS sickness ratings from the last trial and the number of trials completed by each participant were analyzed. We used the FMS sickness ratings from the last trial due to the sickness ratings

becoming severe with increasing exposure time, so the FMS sickness ratings from the last trial best-reflect resistance to VRMS. We removed outliers (if applicable) by Matlab built-in function *rmoutliers(data,'quartiles')* and statistical analysis was performed using SPSS (version 28.0.0.0). Due to the data not meeting the requirement of equal variance assumption a Welch's independent sample t-test was performed to analyze between-group differences. Additionally, effect size for Cohen's d was calculated where Cohen's d has following categories: small effect size ($d=0.2-0.5$), medium effect size ($d=0.5-0.8$) and large effect size ($d>0.8$) [22].

3.5 EEG Data Analysis

Since both PIVC and PIC areas have no clear remapped EEG electrode positions, parietal cortex can be thought to be reflected in electrodes on P3 and P4 [23], [24], due to the parietal cortex having anatomical connections with both areas [16], [25]. Therefore, in the following sections, our EEG results on P3 and P4 reflect estimated results about the left and right PIVC+. Regarding TPJ, we used CP5 and CP6 based on [26], [27], thus we focused on these four EEG sites throughout the study.

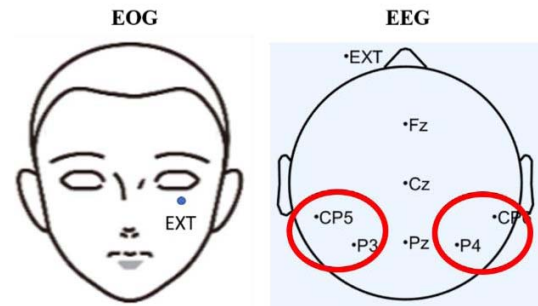


Figure 4: The EEG regions of our interest (circled by the red circle)

Fig. 4 shows the EEG map we used where the EXT site was used to collect a single-channel electrooculography (EOG) signals as a reference noise in independent component analysis (ICA) in order to better reduce eye movement noise in EEG signals. A low-pass filter with a cutoff frequency of 40 Hz and a high-pass filter with a cutoff frequency of 0.1 Hz were applied to remove power line noise and direct current drift, respectively. The filtered EEG data were then corrected using the mean of each channel and EOG-based ICA. Then, for each participant's last trial, relative band power (RBP, the unit is %) in each frequency band (δ :0.1-3Hz, θ :4-7Hz, α :8-12Hz and β : 13-20Hz [28]) at both left and right parietal cortex and TPJ regions were calculated for ensuing statistical analyses and drawing corresponding scalp topographies. The RBP in each band and each region was calculated by dividing the FFT power of one EEG band by the sum of the FFT power of all four EEG bands (δ , θ , α and β) and subtracted by grand average of all regions by Matlab. The RBP calculated in this way provided a means to minimize the possibility that the assessment of EEG biomarkers was confounded by individual differences in the generation of EEG signals. Also, similar to behavioral data analysis, after the removal of outliers by Matlab, the SPSS (version 28.0.0.0)-based regular or Welch's independent sample t-tests with Cohen's d were implemented to compare the between-group RBP in each frequency band. Since 4 EEG frequency bands and 4 EEG electrodes generated 4*4 RBP features for pairwise comparisons, Benjamini-Hochberg false discovery rate (FDR) [29] was used to correct all p values originally calculated by t-test. The tool we used to implement Benjamini-Hochberg FDR is SPSS STATS

PADJUST package. Scalp topographies were drawn using EEGLab v2020.0. (an open-source MATLAB plugin developed by Swartz Center for Computational Neuroscience; www.sccn.ucsd.edu/eeqlab). Note, the data collected from Fz, Cz and Pz were not this paper's focus but used for creating scalp topographies.

3.6 Correlation Analysis of EEG and Behavioral Data

In order to confirm that the discovered brain patterns were indeed associated with VRMS, Pearson correlation analyses of RBP and FMS ratings was implemented by SPSS ver 28.0.0.0.

4 RESULTS

The 10 VRMS-resistant participants showed certain enhanced low-frequency activity (that is, 4-7Hz theta activity) in the left parietal cortex region if compared to the 10 VRMS-susceptible participants. According to sensory-conflict theory [5], this difference in brain pattern can be used to generate new experimental hypotheses including: 1) whether the theta activity found in the VR-resistant individuals acted like a negotiator to compensate the mismatched vestibular sensory inputs before they are integrated with visual sensory inputs together and registered into the brain's *comparator*?; or 2) based on sensory-conflict theory-derived multisensory reweighting theory [30], vestibular sensory inputs were down-weighted and visual ones were up-weighted by the theta activity, then the greater the difference between the two weights, the smaller the weight of the signal difference output by the *comparator* (that is, $conflict = (1 - (W_1 - W_2)) * (S_1 - S_2)$, where W and S stand for the weight and sensory input). If these hypotheses can be confirmed, then this anti-VRMS theta activity pattern is the cause of enhanced resistance to VRMS and thus can be mimicked in VRMS-susceptible individuals using transcranial neuromodulation techniques.

4.1 Behavioral Results

4.1.1 The Time Course of Dropouts

As shown in Fig. 5, the first dropouts (N=2) occurred in the VRMS-susceptible group by the end of the 3rd trial which was around 3 minutes after the VRMS-inducing tunnel travel task started. The maximum dropouts were observed by the end of the 7th trial which was about 7 minutes after the tunnel task started, with 4 participants dropping out at this time point, accounting for

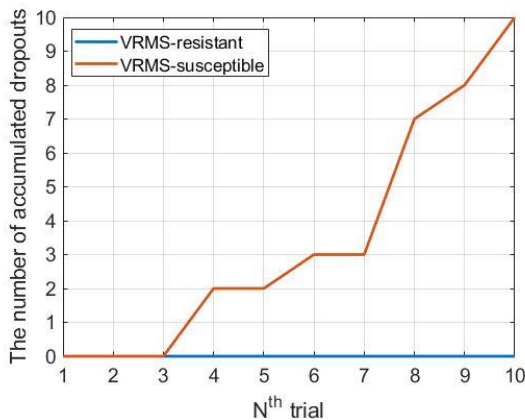


Figure 5: Significant difference found in FMS ratings between VRMS-resistant and -susceptible group

40% of VRMS-susceptible group. The following t-test analysis of the completed number of trials confirmed the statistically significant between-group difference in the tolerable duration of VRMS. Also, the ensuing t-test analysis of sickness ratings indicated that those participants who did not drop out indeed experienced lower VRMS levels.

4.1.2 Number of Completed Trials

As shown in Fig. 6, a significant between-group difference ($t(9)=5.093$, $p<0.001$, Cohen's $d=1.54$) was found for the completed number of trials, with VRMS-resistant participants completing all trials ($M = 10$, $STD = 0$) while VRMS-susceptible participants completed 6.5 trials on average ($STD=2.17$).

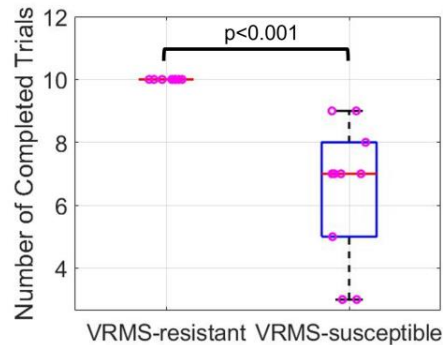


Figure 6: Significant difference found in the completed number of trials between VRMS-resistant and -susceptible group

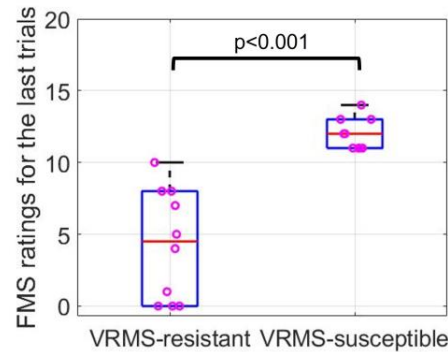


Figure 7: Significant difference in FMS ratings between VRMS-resistant and -susceptible group

4.1.3 FMS Ratings

As shown in Fig. 7, a significant between-group difference ($t(10.652)=-6.033$, $p<0.001$, Cohen's $d=2.911$) was found for FMS ratings, with for the VRMS-resistant participants experiencing lower levels of VRMS ($M=4.3$, $STD=3.86$) compared to VRMS-susceptible participants ($M=12$, $STD=1.118$).

4.0 Results

We found that RBP(theta) was significantly enhanced in the left parietal cortex represented by electrode P3 in VRMS-resistant

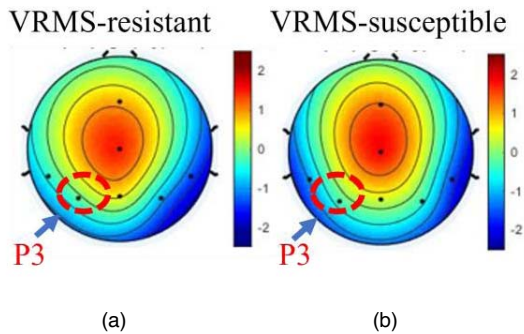


Figure 8: Grand average of values of RBP(theta) in (a) VRMS-resistant and (b) -susceptible group.

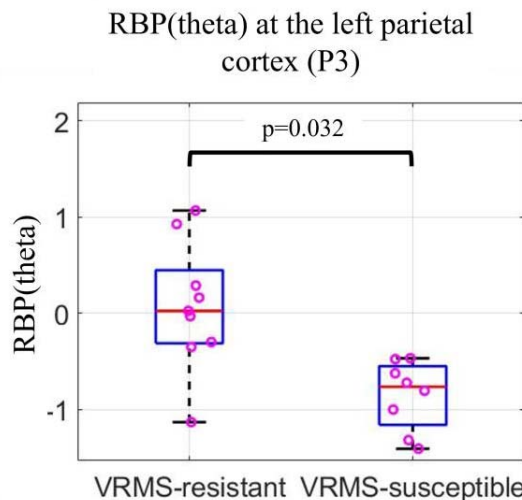


Figure 9: Boxplots (data distribution) of P3-RBP(theta) of all participants.

group ($M=-0.072$, $STD=0.667$) compared to VRMS-susceptible group ($M=-0.855$, $STD=0.361$) with $p=0.032$ and a medium effect size ($d'=0.546$). This result indicates that the VRMS-resistant group experienced enhanced theta brain activities in the left PIVC+ region while watching tunnel travel compared to the VRMS-susceptible group, see Fig. 8 the topographies of grand average of RBP(theta) as well as Fig. 9 the boxplots (data distribution) of RBP(theta) of all participants. We did not find other significant results in other EEG frequency bands and regions.

4.3 Correlates of FMS ratings and EEG Results

A significant Pearson correlation with FMS ratings was found for RBP(theta) at the left parietal cortex as well with $r=-0.523$ and $p=0.031$ as shown in Fig. 10. The trial-by-trial (that is, minute-by-minute) topographies of RBP(theta) from one VRMS-resistant and one VRMS-susceptible participant are shown in Fig. 11 respectively. For the VRMS-resistant participant we can see clearly that the overall trend of increased activation in the left PC comes with little-to-no FMS ratings. Particularly, as shown in the

red square, the only rating that is larger than zero during the entire experiment was reported after the 7th trial, but as theta power intensified, the rating backed to zero again until the end of the experiment; while for the VRMS-susceptible participant, the overall decreased theta activity in the left PC comes with increased FMS ratings until it reaches the pre-defined ethical threshold (thus, this participant completed 6 trials out of 10 trials and then dropped out). Also, based on the scalp topographies, we observed that regardless of the VRMS-resistant and -susceptible by Fz) were not enhanced during the whole procedure of VRMS induction. This is a good sign as it suggests that the differences in VRMS resistance were indeed attributed to parietal cortex regions rather than a volume conduction phenomenon produced by theta activities in other regions, for example, enhanced frontal cognitive processing also could reduce VRMS symptoms [11], and the theta activity in the front midline happens to be a well-established EEG-based indicator of cognitive processing [31].

5 DISCUSSION

5.1 The source of discovered theta pattern (Left PIC?)

The neural mechanisms underlying traditional motion sickness resistance or susceptibility remain largely unclear, not to mention emerging visually-induced motion sickness, like VRMS in this study. A recent resting-state functional magnetic resonance imaging (fMRI) study suggests that there may be a left parietal dominance in susceptibility to motion sickness [32]. The authors found that motion sickness-resistant individuals have greater negative functional connectivity between the left PIC and primary visual cortex area while motion sickness-susceptible individuals show co-activation of the two regions, meaning that motion sickness-resistant individuals may have reduced visual-vestibular mismatch through better reciprocal visual-vestibular interactions (or reweighting in our view, see below) while motion sickness-susceptible individuals have poorer visual-vestibular interactions thus may lead to fierce sensory conflict.

Even though this fMRI study defined the high/low VRMS susceptibility based on self-reports of questionnaires rather than actual data like ours, these findings and authors' speculations still opened a door to explain our findings here. We speculate that our discovered enhanced theta activity in the left PC (P3) was the explicit presentation of the specific left PIC (rather than PIVC in the PIVC+) activity on our scalp area. Specifically, we speculate that before the mismatched visual-vestibular sensory inputs were transmitted to the TPJ, the theta-inducing source in the left PIC was enhanced to actively increase the weights allocated to visual sensory inputs or alternatively to actively decrease the weights allocated to vestibular sensory inputs based on sensory-conflict theory-derived reweighting theory [30]. According to this theory the sensory inputs with more weights can increase the reliability and certainty of those sensory inputs (e.g., the visual sensory inputs in this study) and thus help our brain *ignore* other sensory inputs (e.g., the vestibular sensory inputs in this study) and reduce the difficulty of making final decisions when a sensory conflict exist. It is especially pertinent that visual optic flow-sensitive areas are just in the PC which has anatomical connections that terminate in the region where PIC is located [16].

5.2 Why theta activity stood out?

The best way to answer this question is to replicate what we have done here using fMRI-compatible VR goggles and simultaneous EEG-fMRI recordings. This is our future direction. But based on the existing literature, we still can find some clues to explain why

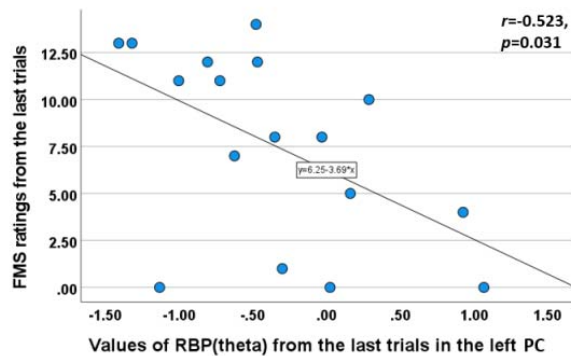


Figure. 10: Significant Pearson correlation found between FMS ratings and RBP(theta) in the left PC

theta activity stood out in the present work. In cognitive neuroscience, theta activity is a well-established biomarker to represent inhibition ability in cognitive processing [33]–[36]. Specifically, participants in a visual Go-NoGo paradigm tended to show enhanced theta activity in NoGo trials if compared to Go trials, where Go trials refer to those trials during which participants were required to cognitively respond while NoGo trials refer to those trials during which participants were required to cognitively inhibit their response. Participants who performed successful inhibition ability in NoGo trials showed greater theta spike than those in Go trials. Therefore, we speculate that theta activity in PIC here has a similar inhibitory effect. As mentioned above, this inhibitory effect is either presented in an indirect way of increasing the weights of visual sensory inputs or in a direct way of decreasing the weights of vestibular sensory inputs. One study supports the possibility of direct inhibition a bit more, because the authors found that cathodal transcranial direct current stimulation (tDCS) applied on PC (represented by P3 which is exactly the same location as the present work) could mitigate traditional motion sickness induced by a rotary chair [24] and cathodal tDCS is a well-established neurostimulation approach to inhibit a brain area [37]. Unfortunately, the authors did not record EEG signals under the condition of cathodal tDCS at P3, which could have helped support our speculation here.

5.3 The Significance for Future Studies

Our finding suggests that it is necessary to investigate the causal relationship between RBP(theta) in the left parietal cortex and the severity of VRMS with non-invasive transcranial electrostimulation techniques in the future (such as tACS and tDCS). This is because they are the current state-of-the-art ways to probe the causal involvement of newly discovered neural biomarkers during a brain state problem, like VRMS. If the causal relationship can be confirmed, then a new VRMS therapy aimed at mimicking the enhanced theta activity presented at the left parietal cortex can be developed, which will be a human-centric solution for VRMS without the need to re-design existing VR contents. Note that transcranial electrostimulation techniques may induce side effects including scalp itching, tingling, burning sensation, phosphenes and so on, and are therefore not suitable for everyone. Also, gel/paste-based wet neurostimulation electrodes may produce some practical hurdles in real-world settings.

However, from the point of view of scientific research, once the causality between our discovered EEG biomarker and the severity of VRMS is established, then we can explore the feasibility of using more user-friendly neural entrainment techniques as real-world-oriented alternatives, like music [38], to achieve the same or comparable goal.

5.4 Limitations

Deep brain activity patterns are undetectable by EEG, thus it remains unclear what the deep brain activity patterns look like in VRMS-resistant people. This is especially pertinent given that deep brain areas are associated with some early signs of visually-induced motion sickness [39]. Also, it is still not clear whether findings in the present study represent the causes or consequences of enhanced resistance to VRMS, thus we suggest that future work should use transcranial alternating current stimulation to probe the causal links between our findings and the severity of VRMS. In addition, we are unable to explain what reasons facilitated this kind of anti-VRMS pattern. Although we excluded professional video game players by setting constraints on the duration of gameplay experienced, there might be other hidden reasons in daily life to enhance the resistance to VRMS that we do not know about. For example, one of our VRMS-resistant participants told us that they used to read a lot on the bus or in a car during their daily commute. Another VRMS-resistant participant noted that they have 16 years of experience in practicing Judo which requires a great deal of spatial awareness and being in control of the body at any time. So, are these in-car activities and sports training a kind of adaptation training that can enhance the resistance to VRMS? Future studies either can take these factors into consideration to set the exclusion criteria if the research target is the general population, or focus on these specific populations if causal link between adaptation training and VRMS is the research question. Both research directions are motivated by our findings.

6 CONCLUSION

This paper investigated the differences in EEG-based brain activity patterns between young adults who are relatively resistant and susceptible to VRMS. We found that RBP(theta) in the left parietal cortex represented by P3 was enhanced in VRMS-resistant group compared to VRMS-susceptible group. This finding comes with a medium effect size and is supported by a significant correlation with VRMS sickness ratings. Then, we discussed why we believe the identified left parietal cortex is a reasonable area to generate an anti-VRMS pattern according to prior knowledge of the PIC and provided speculation about the specific function of RBP(theta) in the context of sensory-conflict theory-derived multisensory reweighting theory as well as cognitive neuroscience-based inhibitory effect.

Acknowledgement

This project has received funding from the European Research Council (ERC) under the European Union’s Horizon 2020 research and innovation programme (No. 835197) and the National Natural Science Foundation of China (No. 61901264). A special thanks to Prof. Ian M. Thornton of the Department of Cognitive Science, University of Malta, for his help designing the tunnel travel task used in this study.

REFERENCES

- [1] S. Nam, K.-M. Jang, M. Kwon, H. K. Lim, and J. Jeong, ‘Electroencephalogram microstates and functional connectivity of cybersickness’, *Frontiers in Human Neuroscience*, vol. 16, 2022,

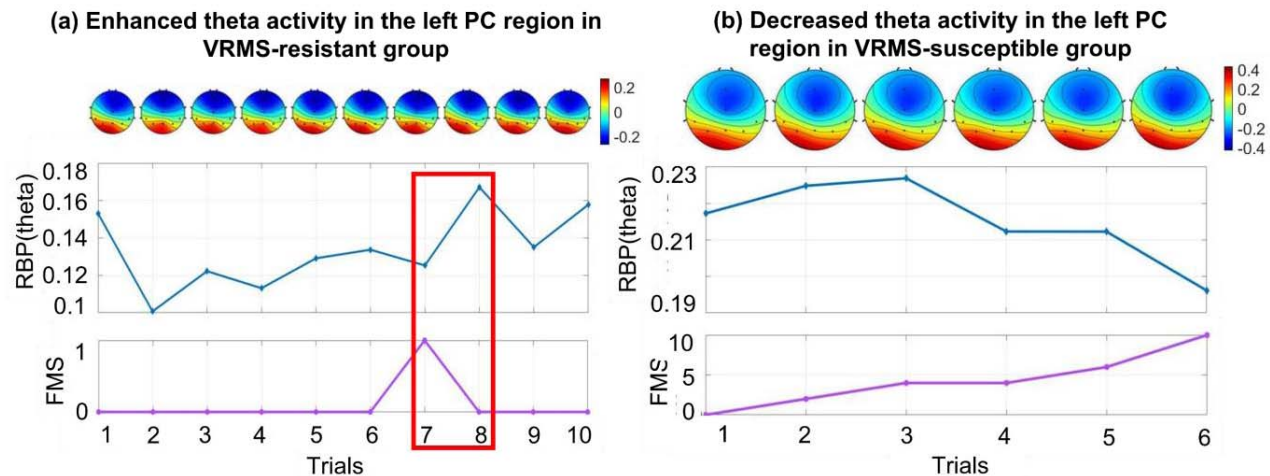


Figure 11: Examples of trial-by-trial analyses of (a) VRMS-resistant and (b) -susceptible participants where the scalp topographies present the values of RBP(theta) from all 7 EEG channels (Fz, Pz, Cz, P3, P4, CP5 and CP6), the blue and purple curves refer to the specific values of RBP(theta) in the left PC (P3) and corresponding FMS ratings from each trial, respectively.

- Accessed: Oct. 11, 2022. [Online]. Available: <https://www.frontiersin.org/articles/10.3389/fnhum.2022.857768>
- [2] S. Weech and N. F. Troje, 'Vection Latency Is Reduced by Bone-Conducted Vibration and Noisy Galvanic Vestibular Stimulation', *Multisens Res*, vol. 30, no. 1, pp. 65–90, 2017, doi: 10.1163/22134808-00002545.
 - [3] J. Tauscher *et al.*, 'Exploring neural and peripheral physiological correlates of simulator sickness', *Comput Anim Virtual Worlds*, vol. 31, no. 4–5, Jul. 2020, doi: 10.1002/cav.1953.
 - [4] R. Islam, Y. Lee, M. Jaloli, I. Muhammad, D. Zhu, and J. Quarles, 'Automatic Detection of Cybersickness from Physiological Signal in a Virtual Roller Coaster Simulation', in *2020 IEEE Conference on Virtual Reality and 3D User Interfaces Abstracts and Workshops (VRW)*, Mar. 2020, pp. 648–649. doi: 10.1109/VRW50115.2020.00175.
 - [5] J. T. Reason, 'Motion sickness—some theoretical considerations', *International Journal of Man-Machine Studies*, vol. 1, no. 1, pp. 21–38, Jan. 1969, doi: 10.1016/S0020-7373(69)80009-X.
 - [6] M. Nürnberg, C. Klingner, O. W. Witte, and S. Brodoehl, 'Mismatch of Visual-Vestibular Information in Virtual Reality: Is Motion Sickness Part of the Brains Attempt to Reduce the Prediction Error?', *Frontiers in Human Neuroscience*, vol. 15, 2021, Accessed: Oct. 11, 2022. [Online]. Available: <https://www.frontiersin.org/articles/10.3389/fnhum.2021.757735>
 - [7] G. Li *et al.*, 'Multimodal Biosensing for Vestibular Network-Based Cybersickness Detection', *IEEE Journal of Biomedical and Health Informatics*, pp. 1–1, 2021, doi: 10.1109/JBHI.2021.3134024.
 - [8] C. Liao, S. Tai, R. Chen, and H. Hendry, 'Using EEG and Deep Learning to Predict Motion Sickness Under Wearing a Virtual Reality Device', *IEEE Access*, vol. 8, pp. 126784–126796, 2020, doi: 10.1109/ACCESS.2020.3008165.
 - [9] D. Jeong, S. Yoo, and J. Yun, 'Cybersickness Analysis with EEG Using Deep Learning Algorithms', in *2019 IEEE Conference on Virtual Reality and 3D User Interfaces (VR)*, Mar. 2019, pp. 827–835. doi: 10.1109/VR.2019.8798334.
 - [10] G. Li, O. Onuoha, M. McGill, S. Brewster, C. P. Chen, and F. Pollick, 'Comparing Autonomic Physiological and Electroencephalography Features for VR Sickness Detection Using Predictive Models', in *2021 IEEE Symposium Series on Computational Intelligence (SSCI)*, 2021, pp. 01–08.
 - [11] K. Pohlmann, J. F. H. A. Maior, L. O'Hare, A. Parke, A. Landowska, and P. Dickinson, 'I think I don't feel sick: Exploring the Relationship Between Cognitive Demand and Cybersickness in Virtual Reality using fNIRS'. Hamburg, Germany, Apr. 23, 2023.
 - [12] G. Li and M. Adeel Khan, 'Deep Learning on VR-Induced Attention', in *2019 IEEE International Conference on Artificial Intelligence and Virtual Reality (AIVR)*, Dec. 2019, pp. 163–1633. doi: 10.1109/AIVR46125.2019.00033.
 - [13] T. G. Dobie, *Motion sickness: a motion adaptation syndrome*. 2019. Accessed: Jun. 21, 2020. [Online]. Available: <https://search.ebscohost.com/login.aspx?direct=true&scope=site&db=nlebk&db=nlabk&AN=2015249>
 - [14] J. Ventre-Dominey, 'Vestibular function in the temporal and parietal cortex: distinct velocity and inertial processing pathways', *Front Integr Neurosci*, vol. 8, p. 53, 2014, doi: 10.3389/fnint.2014.00053.
 - [15] P. H. Donaldson, N. J. Rinehart, and P. G. Enticott, 'Noninvasive stimulation of the temporoparietal junction: A systematic review', *Neurosci Biobehav Rev*, vol. 55, pp. 547–572, Aug. 2015, doi: 10.1016/j.neubiorev.2015.05.017.
 - [16] S. M. Frank and M. W. Greenlee, 'The parieto-insular vestibular cortex in humans: more than a single area?', *Journal of Neurophysiology*, vol. 120, no. 3, pp. 1438–1450, Sep. 2018, doi: 10.1152/jn.00907.2017.
 - [17] B. Keshavarz and H. Hecht, 'Validating an efficient method to quantify motion sickness', *Hum Factors*, vol. 53, no. 4, pp. 415–426, Aug. 2011, doi: 10.1177/0018720811403736.
 - [18] R. S. Kennedy, N. E. Lane, K. S. Berbaum, and M. G. Lilienthal, 'Simulator Sickness Questionnaire: An Enhanced Method for Quantifying Simulator Sickness', *The International Journal of Aviation Psychology*, vol. 3, no. 3, pp. 203–220, Jul. 1993, doi: 10.1207/s15327108ijap0303_3.
 - [19] F. Caniard, H. H. Bühlhoff, and I. M. Thornton, 'Action can amplify motion-induced illusory displacement', *Frontiers in Human Neuroscience*, vol. 8, 2015, Accessed: Sep. 23, 2022. [Online]. Available: <https://www.frontiersin.org/articles/10.3389/fnhum.2014.01058>
 - [20] G. Li, J. A. Anguera, S. V. Javed, M. A. Khan, G. Wang, and A. Gazzaley, 'Enhanced Attention Using Head-mounted Virtual Reality', *J Cogn Neurosci*, vol. 32, no. 8, pp. 1438–1454, Aug. 2020, doi: 10.1162/jocn_a_01560.
 - [21] G. Li, S. Zhou, Z. Kong, and M. Guo, 'Closed-Loop Attention Restoration Theory for Virtual Reality-Based Attentional Engagement Enhancement', *Sensors (Basel)*, vol. 20, no. 8, p. 2208, Apr. 2020, doi: 10.3390/s20082208.
 - [22] J. Cohen, 'A power primer', *Psychol Bull*, vol. 112, no. 1, pp. 155–159, Jul. 1992, doi: 10.1037//0033-2909.112.1.155.
 - [23] J. Dowsett, C. S. Herrmann, M. Dieterich, and P. C. J. Taylor, 'Shift in lateralization during illusory self-motion: EEG responses to

- visual flicker at 10 Hz and frequency-specific modulation by tACS', *Eur J Neurosci*, vol. 51, no. 7, pp. 1657–1675, Apr. 2020, doi: 10.1111/ejn.14543.
- [24] Q. Arshad *et al.*, 'Electrocortical therapy for motion sickness', *Neurology*, vol. 85, no. 14, pp. 1257–1259, Oct. 2015, doi: 10.1212/WNL.0000000000001989.
- [25] M. Uesaki, H. Takemura, and H. Ashida, 'Computational neuroanatomy of human stratum proprium of interparietal sulcus', *Brain Struct Funct*, vol. 223, no. 1, pp. 489–507, 2018, doi: 10.1007/s00429-017-1492-1.
- [26] N. Takeuchi, T. Mori, Y. Suzukamo, and S.-I. Izumi, 'Modulation of Excitability in the Temporoparietal Junction Relieves Virtual Reality Sickness', *Cyberpsychol Behav Soc Netw*, vol. 21, no. 6, pp. 381–387, Jun. 2018, doi: 10.1089/cyber.2017.0499.
- [27] A. Kyriakareli, S. Cousins, V. E. Pettorossi, and A. M. Bronstein, 'Effect of transcranial direct current stimulation on vestibular-ocular and vestibulo-perceptual thresholds', *Neuroreport*, vol. 24, no. 14, pp. 808–812, Oct. 2013, doi: 10.1097/WNR.0b013e3283646e65.
- [28] Y.-C. Chen *et al.*, 'Spatial and temporal EEG dynamics of motion sickness', *NeuroImage*, vol. 49, no. 3, pp. 2862–2870, Feb. 2010, doi: 10.1016/j.neuroimage.2009.10.005.
- [29] Y. Benjamini and Y. Hochberg, 'Controlling the False Discovery Rate: A Practical and Powerful Approach to Multiple Testing', *Journal of the Royal Statistical Society. Series B (Methodological)*, vol. 57, no. 1, pp. 289–300, 1995, Accessed: Jan. 18, 2023. [Online]. Available: <https://www.jstor.org/stable/2346101>
- [30] M. Gallagher and E. R. Ferrè, 'Cybersickness: a Multisensory Integration Perspective', *Multisens Res*, vol. 31, no. 7, pp. 645–674, Jan. 2018, doi: 10.1163/22134808-20181293.
- [31] J. A. Anguera *et al.*, 'Video game training enhances cognitive control in older adults', *Nature*, vol. 501, no. 7465, Art. no. 7465, Sep. 2013, doi: 10.1038/nature12486.
- [32] H. Sakai *et al.*, 'Left parietal involvement in motion sickness susceptibility revealed by multimodal magnetic resonance imaging', *Hum Brain Mapp*, vol. 43, no. 3, pp. 1103–1111, Nov. 2021, doi: 10.1002/hbm.25710.
- [33] M. R. Brier *et al.*, 'Frontal theta and alpha power and coherence changes are modulated by semantic complexity in Go/NoGo tasks', *Int J Psychophysiol*, vol. 78, no. 3, pp. 215–224, Dec. 2010, doi: 10.1016/j.ijpsycho.2010.07.011.
- [34] V. Müller and A. P. Anokhin, 'Neural synchrony during response production and inhibition', *PLoS One*, vol. 7, no. 6, p. e38931, 2012, doi: 10.1371/journal.pone.0038931.
- [35] K. Yamanaka and Y. Yamamoto, 'Single-trial EEG power and phase dynamics associated with voluntary response inhibition', *J Cogn Neurosci*, vol. 22, no. 4, pp. 714–727, Apr. 2010, doi: 10.1162/jocn.2009.21258.
- [36] J. Anguera, K. Lyman, T. Zanto, J. Bollinger, and A. Gazzaley, 'Reconciling the influence of task-set switching and motor inhibition processes on stop signal after-effects', *Frontiers in Psychology*, vol. 4, 2013, Accessed: Oct. 12, 2022. [Online]. Available: <https://www.frontiersin.org/articles/10.3389/fpsyg.2013.00649>
- [37] M. A. Nitsche and W. Paulus, 'Excitability changes induced in the human motor cortex by weak transcranial direct current stimulation', *J Physiol*, vol. 527, no. Pt 3, pp. 633–639, Sep. 2000, doi: 10.1111/j.1469-7793.2000.t01-1-00633.x.
- [38] S. Nozaradan, 'Exploring how musical rhythm entrains brain activity with electroencephalogram frequency-tagging', *Philosophical Transactions of the Royal Society B: Biological Sciences*, vol. 369, no. 1658, p. 20130393, Dec. 2014, doi: 10.1098/rstb.2013.0393.
- [39] V. Napadow *et al.*, 'The Brain Circuitry Underlying the Temporal Evolution of Nausea in Humans', *Cereb Cortex*, vol. 23, no. 4, pp. 806–813, Apr. 2013, doi: 10.1093/cercor/bhs073.